

Determining the Chemical Exchange Saturation Transfer (CEST) Behavior of Citrate and Spermine under In Vivo Conditions

Meer Basharat, Nandita M. deSouza, Harold G. Parkes, and Geoffrey S. Payne*

Purpose: To estimate the exchange rates of labile ^1H in citrate and spermine, metabolites present in prostatic secretions, to predict the size of the citrate and spermine CEST effects in vivo.

Methods: CEST z-spectra were acquired at high-field [11.7 Tesla (T)] from citrate and spermine solutions at physiological pH (6.5) using saturation power $6 \mu\text{T}$. CEST was performed at different temperatures to determine exchange regimes (slow, intermediate or fast). For low pH solutions of spermine, exchange rates were estimated from resonance line width, fitting z-spectra using the Bloch equations incorporating exchange, and using quantifying exchange using saturation time experiments (QUEST). These rates were extrapolated to physiological pH.

Results: Citrate showed little CEST effect at pH 6.5 and temperature (T) = 310 K (maximum $0.001\% \text{ mM}^{-1}$), indicating fast exchange, whereas spermine showed greater CEST effects (maximum $0.2\% \text{ mM}^{-1}$) indicating intermediate-to-fast exchange. Extrapolating data acquired from low pH spermine solutions predicts exchange rates at pH 6.5 and T of 310 K of at least $2 \times 10^4 \text{ s}^{-1}$.

Conclusion: Citrate and spermine show minimal CEST effects at 11.7T even using high saturation power. These effects would be much less than 2% at clinical field-strengths due to relatively faster exchange and would be masked by CEST from proteins. **Magn Reson Med 76:742–746, 2016. © 2015 The Authors. Magnetic Resonance in Medicine published by Wiley Periodicals, Inc. on behalf of International Society for Magnetic Resonance in Medicine. This is an open access article under the terms of the Creative Commons Attribution License, which permits use, distribution and reproduction in any medium, provided the original work is properly cited.**

Key words: CEST; spermine; citrate; exchange; QUEST

chemical exchange saturation transfer (CEST), which interrogates ^1H nuclei in molecules such as metabolites and proteins (pool **s**), which are exchanging with ^1H nuclei in water (pool **w**). CEST contrast is produced by applying a saturation pulse at the resonance frequency of the ^1H in pool **s** (ν_s). The saturated ^1H nuclei in pool **s** then exchange with unsaturated ^1H nuclei in water at rate k_{sw} . After successive saturation-and-exchange events the water signal is attenuated.

CEST contrast is advantageous for measuring low-concentration ^1H pools because the water signal attenuation may be tens or hundreds fold larger than the inherent MR signal from these nuclei. CEST has been applied to image the distributions of myo-inositol (1), creatine (2) and glutamate (3) in humans. In the prostate, CEST effects have previously been attributed to the ^1H nuclei of protein amides (4). However, the glandular metabolites citrate and spermine (normal concentrations of 40 mM and 10 mM (5), and containing labile -OH and $-\text{NH}_x$ groups, respectively, see Supporting Figure S1, which is available online) are large potential CEST sources in the prostate. While the concentrations of these metabolites decrease significantly from normal in benign and malignant prostate disease (6), it is not always easy to visualize them using MR spectroscopy due to spectral overlap and lipid contamination. Because characterization, evaluation, and optimization of the CEST effects of citrate and spermine have not yet been reported, in this study the exchange conditions and estimates of the chemical exchange rates of ^1H in citrate and spermine with water were determined. This then provides predictions for CEST behaviors at physiological pH and temperature and relevant field-strengths.

INTRODUCTION

MRI examinations typically create contrast between tissues in the body by exploiting the different NMR relaxation times of water ^1H nuclei. An alternative contrast mechanism is

CRUK Cancer Imaging Centre, Institute of Cancer Research and Royal Marsden NHS Foundation Trust, Downs Road, Sutton, Surrey United Kingdom

*Correspondence to: Geoffrey Payne, Ph.D., MRI Unit, Royal Marsden NHS Foundation Trust, Downs Road, Sutton, Surrey, SM2 5PT, UK. E-mail: geoffrey.payne@icr.ac.uk

Received 30 January 2015; revised 20 August 2015; accepted 29 August 2015

DOI 10.1002/mrm.25997

Published online 15 October 2015 in Wiley Online Library (wileyonlinelibrary.com).

© 2015 The Authors. Magnetic Resonance in Medicine published by Wiley Periodicals, Inc. on behalf of International Society for Magnetic Resonance in Medicine. This is an open access article under the terms of the Creative Commons Attribution License, which permits use, distribution and reproduction in any medium, provided the original work is properly cited.

© 2015 Wiley Periodicals, Inc.

METHODS

Theoretical Background

The amount of CEST that occurs from a ^1H species depends on its concentration, chemical exchange rate with ^1H in water and the relaxation rates. Very slow exchange causes little CEST. CEST is also diminished at high exchange rates at which the resonances of exchanging ^1H species coalesce because the CEST saturation pulse is unable to selectively saturate pool **s** without some direct saturation of pool **w**. The chemical exchange rate for coalescence is given by (7)

$$k_{sw} = 2^{-1/2} \pi \Delta\nu \approx 2.22 \Delta\nu \quad [1]$$

where $\Delta\nu$ is the chemical shift difference, $\nu_s - \nu_w$. The greatest CEST effects, therefore, occur for ^1H with

intermediate exchange rates, $k_{sw} < 2.22\Delta\nu$ (8). For example, at field-strength 7 Tesla (T) the ^1H exchange rate in glutamate [$k_{sw} = 875\text{s}^{-1}$ (3)] is nearly optimal for CEST (at 7T, $\Delta\nu = 894\text{s}^{-1}$, so $k_{sw} = 0.98\Delta\nu$).

Methods to measure the chemical exchange rates of slowly-exchanging ^1H include measurement of the resonance linewidth (9), fitting the Z spectra of the full Bloch equations including exchange (10), and using the method of quantifying exchange using saturation time (QUEST, see below) (9). Exchange rates at different pH values can be estimated using (11);

$$k_{sw}(\text{pH}) = k_0 + k_a 10^{(-\text{pH})} + k_b 10^{(\text{pH}-\text{pK}_w)} \quad [2]$$

where k_0 is the spontaneous exchange rate, k_a is the acid-catalyzed exchange constant, k_b is the base-catalyzed exchange constant, and pK_w is the water ionization constant [13.62 at 310 K (12)]. k_{sw} has a minimum value at $\text{pH} = \frac{1}{2}(\log_{10}(k_a/k_b) + \text{pK}_w)$, which commonly occurs at pH 3–4 (13), and increases for all other pH values.

Quantifying Exchange Using Saturation Time

Under many conditions, the asymmetric magnetization transfer ratio (MTR_{asym}) can be shown to have the form (9):

$$\text{MTR}_{\text{asym}} = (S_w(-\Delta) - S_w(+\Delta)) / S_{0w} = p(1 - e^{-qt}) \quad [3]$$

where p and q are constants, t is the saturation pulse length and $S_w(\Delta)$ is the attenuated water signal due to saturation at frequency offset Δ . Parameter q is dependent on k_{sw} , the water relaxation rate (R_{1w}) and the relative numbers of ^1H in pool i involved in exchange at irradiation frequency offset Δ (9);

$$k_{sw}(\Delta) = (q(\Delta) - R_{1w}) * (n_w/n_s(\Delta)). \quad [4]$$

Exchange must be relatively slow. In the QUEST method (9) $S_w(\Delta)$ is measured at a range of saturation durations, t , with Δ set to the frequency of the exchanging hydrogens (and to the corresponding frequency on the other side of water). Fitting Eq. [3] to the data yields parameter q ; k_{sw} is obtained using Eq. [4].

Experimental Procedures

Spectra were acquired using a 5 mm BBO probe in a 500 MHz vertical bore system (Bruker) to exploit the high values of $\Delta\nu$ and so increase the signal change from the CEST effect. Chemical shift offsets are given relative to water unless otherwise stated.

Resonance Offset Determination

A total of 100 mM citrate was scanned at 310 and 277 K, pH 6.5 and 2.0, with 64 repetitions and 16k complex points over 10 kHz bandwidth. The 20 mM spermine was scanned at 301 K, pH 3.1 and 4.3, with 128 repetitions and 16k complex points over 6 kHz bandwidth.

Exchange Regime Determination

To determine the exchange regime (slow, intermediate or fast), the relationship of chemical exchange rate with

temperature was exploited. At constant pH, k_{sw} increases with increasing temperature (Eyring equation). Increased k_{sw} produces more CEST if k_{sw} is slow at the lower temperature, but reduced CEST if already in intermediate exchange and the coalescence condition is approached.

Solutions of 100 mM citrate and 20 mM spermine tetrahydrochloride were studied at physiological pH [6.5 (14)] using sodium hydroxide to achieve the required pH. CEST effects were measured using a saturation time of 1 s and temperatures of 280 K, 295 K and 310 K. A total of 100 mM citrate was also investigated at pH 2.0, 310 K, and with 4 s saturation. Acquisition parameters included 16 repetitions, 20 s repetition time, 16 k complex points, and 6 kHz bandwidth. Saturation was achieved using a continuous-wave block saturation pulse with amplitude 6 μT (255 Hz). The saturation pulse amplitude was verified by measuring the pulse length required for a 90-degree pulse. $S_w(\Delta)$ was measured by integrating the absorption signal from +0.5 to -0.5 ppm relative to water. The attenuation due only to CEST was determined by cancelling out the symmetric direct saturation component of each z-spectrum by calculating the asymmetric magnetization transfer ratio (Eq. [3]).

Average MTR_{asym} was calculated between +1.2 ppm to 0 ppm for citrate (hydroxyl groups expected at approximately +0.8 to +0.6 ppm), and from +5.0 ppm to 0 ppm for spermine (amine groups expected at +3 to +4 ppm). Average MTR_{asym} is analogous to the MTR_{asym} integral used in others studies (15,16) but more intuitively describes the amount of CEST occurring.

Exchange Rate Measurements on Spermine

Exchange rates were estimated from solute peak linewidths, fitting z-spectra to the full Bloch equations using exchange, and using the QUEST method. Spermine solutions at pH 3.1 and 4.3 were measured. These were lower than that of prostatic fluid [pH approximately 6.5 (14)] with the intention of achieving slower exchange rates that are more readily measured.

Linewidth measurements were made using pulse-acquire spectra without water suppression (repetition time of 5.7s, 128 repetitions, other parameters as above). The exchange rate was calculated using (9);

$$k_{sw} = \pi.LW_s - R_{2s}. \quad [5]$$

Z-spectra were acquired by measuring the amplitude of the bulk water signal, $S_w(\Delta)$, after applying saturation at offset frequencies Δ from +5.0 to -5.0 ppm relative to water, in 0.2 ppm increments. The saturation duration was 4 s. S_{0w} was found by performing the measurement using a saturation pulse with offset frequency $\Delta = +20$ ppm. Resulting z spectra were fit using the full Bloch equations including exchange [based on (10) but modified to run in IDL]. B_1 and saturation times were fixed at the values specified above, while the chemical shift offsets, relaxation parameters and exchange rate were fitted to the data. To reduce the number of free parameters, it was assumed that both amine pools had the same values of T_1 , T_2 , and exchange life time.

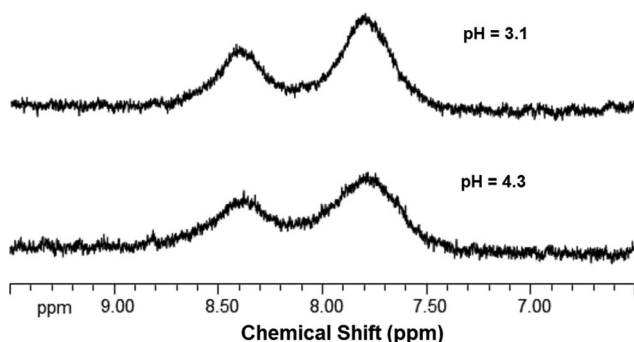


FIG. 1. Pulse-acquire ^1H NMR spectra of spermine at pH 3.1 and 4.3, showing the chemical shift offsets of the amine resonances (relative to TMS; peak positions relative to water are approximately 3.0 and 3.7 ppm). Acquisition parameters included temperature = 310 K, spectral width 6009 Hz, 16 k complex points, TR = 5.73 s, 128 repetitions.

For QUEST measurements, water spectra were acquired with saturation durations of 0, 0.5, 1.0, 2.0, 4.0, 8.0 and 12.0 s at frequency offsets of ± 3.0 ppm relative to water, corresponding to the position of the main resonance peak observed in the pulse-acquire spectra. Plots of MTR_{asym} versus saturation time t were fitted in IDL to find values for p and q using Eq. [3].

R_{1w} was measured by performing inversion-recovery experiments using inversion times, TI, of 1 s to 20 s in 1 s increments, and recovery delay of 15s. Data were fitted using

$$S_w/S_{0w} = 1 - a.e^{(-R_{1w} \cdot \text{TI})}. \quad [6]$$

A 3-mm tube in the 5-mm probe was used to minimize the effects of radiation damping.

Estimation of Exchange Rates at pH 6.5

Exchange rates were extrapolated to pH 6.5 by using $k_{sw}(\text{pH } 3.1)$ and $k_{sw}(\text{pH } 4.3)$ to determine k_0 and k_b in Eq. [2]. The k_a term was omitted because only chemical exchange rates for $\text{pH} > 3$ were considered.

RESULTS

Citrate

No peaks were visible in pulse-acquire spectra of citrate at pH 6.5 and at pH 2.0 except for that from water, even at 277 K. This suggests either fast exchange, or a hydroxyl peak that is within the linewidth of the water resonance. Simulations based on standard exchange line-shape analysis [e.g., Gunther (17)] show that a separate 100 mM resonance at 1 ppm offset, intrinsic linewidth 1 Hz, $B_0 = 11.7\text{T}$, broadens to invisibility for k_{sw} larger than ~ 2000 Hz.

A total of 100 mM citrate solution at pH 6.5 and temperature (T) = 310 K, 295 K, and 280 K demonstrated negligible CEST, with average MTR_{asym} of $0.1\% < 0.01\%$, and $< 0.01\%$, respectively. All these measurements of CEST in citrate are effectively zero, with no significant difference between them. This is consistent with chemical exchange in citrate being in the fast exchange regime at 11.7T and pH 6.5. Likewise, no CEST effects were observed for 100

mM citrate at pH 2.0 and $T = 310$ K, where the exchange rates should have been substantially lower than at pH 6.5 and the same temperature. Because no peaks or CEST effect were observed at any temperature or pH measured, the determination of k_{sw} was not attempted.

Spermine

Pulse-acquire spectra of 20 mM spermine at 310 K and pH 3.1 and 4.3 are shown in Figure 1. The amine resonances are seen at approximately 3.0 and 3.7 ppm relative to water (giving exchange coalescence limits of approximately 3300 and 4100 Hz, respectively). At pH 4.3, the linewidths are 187 Hz and 177 Hz, respectively. Given that R_{2s} is expected to be similar to that of the water ($\sim 1 \text{ s}^{-1}$) the linewidth is dominated by the exchange rate, which using Eq. [5] can be estimated as approximately 590 Hz and 570 Hz, respectively. At pH 3.1, the corresponding estimated exchange rates are 470 Hz and 440 Hz, respectively. The water line widths in these samples were in the range 9.5 to 12.5 Hz.

The 20 mM spermine at pH 6.5 and $T = 310$ K demonstrated a broad CEST effect with average $\text{MTR}_{\text{asym}} = 1.36\%$ (Fig. 2). The amount of CEST from spermine at pH 6.5 increased with decrease in temperature, with average $\text{MTR}_{\text{asym}} = 18.7\%$ at $T = 295$ K and average $\text{MTR}_{\text{asym}} = 24.0\%$ at $T = 280$ K. This increase in CEST with reducing temperature (and hence exchange rate) indicates that chemical exchange in spermine is in the intermediate-to-fast regime at pH 6.5 and field-strength 11.7T.

A full z-spectrum of spermine at pH 4.3 and 310 K using saturation pulses of duration 4 s is shown in Figure 3. The resulting calculated exchange rates were 461 Hz (pH 3.1) and 676 Hz (pH 4.3).

The chemical exchange rates for spermine at an offset frequency of 3.0 relative to water were calculated using QUEST at pH 3.1 and 4.3, with $T = 310$ K. The fitted curves are shown in Figure 4. Equation [6] yielded R_{1w} as 0.207 s^{-1} and 0.208 s^{-1} at pH 3.1 and 4.3, respectively (and “a” as 1.99). With fitted q values of 0.525 and 0.661, and a ratio (n_w/n_s) of 110000/120 (i.e., assuming 6

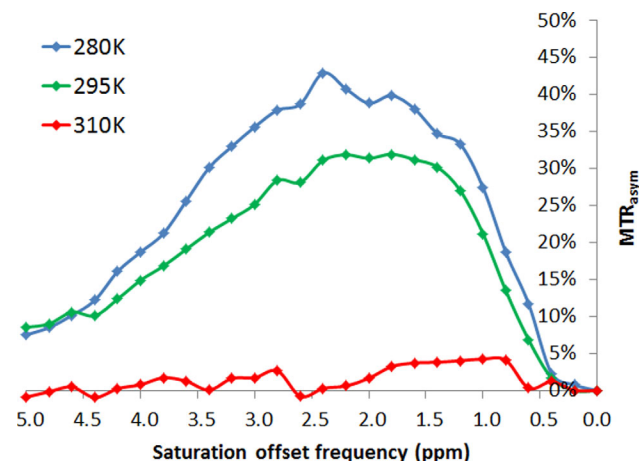


FIG. 2. MTR_{asym} plots from z-spectra acquired from 20 mM solutions of spermine at pH 6.5. The increasing CEST effect at lower temperature (reducing k_{sw}) indicates chemical exchange in the intermediate-to-fast regime at $T = 310$ K

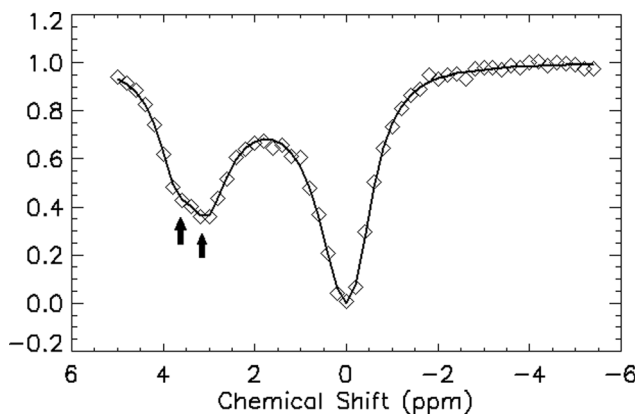


FIG. 3. Z-spectrum obtained from 20 mM spermine at pH 4.3 and at 310 K. Water signals at each time point were acquired with spectral width 6009 Hz, 16 k complex points, repetition time = 22.73 s, and 4 repetitions. The fitted curve was obtained using a 3-pool CEST fitting routine described in Woessner et al (10) but modified for use in IDL.

hydrogen nuclei involved in exchange in 20 mM spermine at this offset) this results in k_{sw} of 291 and 416 Hz, respectively.

The exchange rates measured using the three different methods are summarized in Table 1, together with the predicted exchange rates at pH 6.5 obtained by extrapolation.

DISCUSSION

In this study, no resonance peaks or CEST effects were observed for citrate, even when pH was reduced to 2.0 and temperature to 277 K This is consistent with fast exchange. It is also possible that the resonance peak was so close to water that no peaks could be observed.

For spermine, by decreasing the pH the exchange rate was measured in the slow exchanging regime, and then extrapolated to physiologic pH and faster exchange regimes, using the known $k_{sw}(pH)$ relationship. Results indicated that chemical exchange in spermine is in the intermediate-to-fast exchange regime at 11.7T, for pH 6.5 and temperature of 310 K, with an extrapolated exchange rate of at least $2 \times 10^4 s^{-1}$ (Table 1). This is roughly 10 times faster than chemical exchange rates observed in creatine [$950 s^{-1}$ (2)] and glutamate [$875s^{-1}$ (3)], and well above the coalescence limit (3300 and 4100 Hz for the 3.0 and 3.7ppm peaks, respectively). Such rapid exchange is consistent with the small CEST profile observed for spermine at 310 K (Fig. 2).

In consequence of their rapid exchange rates, neither citrate nor spermine will be likely to contribute to CEST effects in the prostate at clinical field-strengths, as at

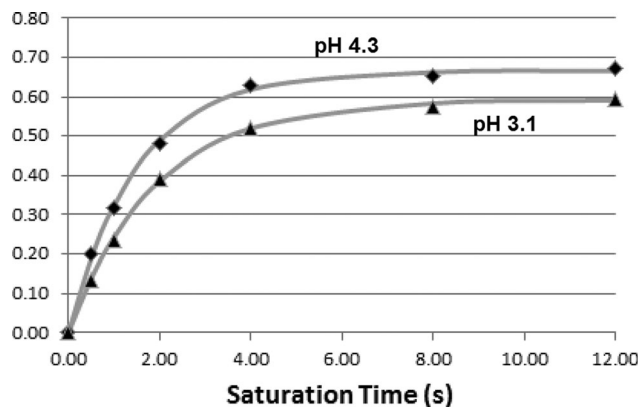


FIG. 4. Quantifying Exchange using Saturation Time (QUEST) fits of spermine CEST at $\Delta = +3.0$ ppm, pH values of 3.1 and 4.3, and at 310 K. Due to base-catalyzed chemical exchange, exchange and CEST are greater at pH 4.3 than at pH 3.1.

lower fields the rate of exchange relative to the chemical shift difference between the 1H nuclei in pools *s* and *w*, will be even larger, with greater coalescence of peaks. CEST effects from exchanging nuclei in other molecules such as proteins are, therefore, predicted to completely conceal the small CEST effects from citrate and spermine in the prostate in vivo.

Conditions which affect the CEST effect from metabolites include saturation power and duration, tissue pH, and relaxation times. A lower saturation power than used in this study (6 μT) would probably reduce the CEST effect but may also reduce direct saturation of the water. The pH of the prostate does vary, but pH 6.5 is at the acidic end of the measured physiological range for prostatic fluid: 6.2–8.0 (14), 6.7 (18), and 6.6 (19); more alkaline pH will elicit faster chemical exchange and even less CEST. While the difference in relaxation characteristics in vivo compared with our solutions will have some effect on the amount of CEST signal anticipated, spermine and citrate are primarily located in the prostatic ducts and are, therefore, relatively mobile with expected relaxation times not greatly different to those in solution.

The three different methods for measuring spermine exchange rates produced values of a similar magnitude but with the QUEST method producing much lower values. The reason for this may be related to the QUEST calculation assuming instantaneous equilibrium (9), a condition which will not be quite valid for metabolites in dilute solution for which T_{2s} is expected to be relatively long. The small uncompensated direct saturation of water may also contribute, as the water linewidths (approximately 10 Hz) suggest that R_{2w} is larger than the 6 Hz limit suggested in (9) to not require correction. However,

Table 1
Summary of Measured Spermine Exchange Rates (pH 3.1 and 4.3), with Extrapolation to pH 6.5^a

Method	k_{sw} (Hz)			Fitted k_b	Fitted k_0
	pH 3.1	pH 4.3	pH 6.5 (extrapolated)	(Hz)	(Hz)
Linewidth	453	572	20,580	2.65×10^{11}	445
Fit to z spectrum	461	676	36,820	4.79×10^{11}	447
QUEST	291	416	21,430	2.79×10^{11}	283

^aThe k_{sw} values calculated from the linewidth measurements were averaged over the two peaks.

the use of MTR_{asym} rather than the proton transfer ratio (9) in the measurement should partially compensate for this. The z-spectrum method uses eight fitted parameters, and is, therefore, probably over-fitted. A full analysis of the interaction of the various parameters in the fit has not been performed, but while the chemical shift offsets are fairly well defined by the minima in the curve, the remaining curvature will include contributions from all relaxation rates as well as the exchange rate, reducing the expected accuracy in each of these. Given these limitations, the simple linewidth measurement may, therefore, be the most accurate. However, all values predict that at physiological pH spermine is unlikely to produce significant CEST signals at clinical field strengths. Because no significant CEST signals were seen in either spermine or citrate solutions at 11.7T and 310 K (Fig. 2), it is not expected that they would be seen in vivo even at field strengths available for preclinical studies.

CONCLUSIONS

Citrate and spermine are glandular metabolites of interest for probing prostate diseases. Both contain labile ^1H groups which in principle may create CEST contrast. Experiments at 11.7T and pH 6.5 found that the CEST effect was less than $0.2\% \text{ mM}^{-1}$ for spermine, and was unmeasurable for citrate. Chemical exchange was determined to be in the fast and intermediate-to-fast exchange regimes for citrate and spermine respectively at 11.7T, under physiological conditions. At clinical field-strengths such as 7T and 3T, these CEST effects would be further reduced due to coalescence of the exchanging ^1H peaks with the bulk water peak. In vivo, these CEST effects are expected to be obscured by CEST from ^1H in proteins and other metabolites.

ACKNOWLEDGMENTS

The authors thank Yann Jamin for his help with using the Bruker NMR system and with acquiring the CEST data, Matthew Orton for help with the IDL fitting routines, and Dr. Dean Sherry of UT Southwestern Medical Center, Dallas, for making available his Matlab code for fitting the z spectra using the Bloch equations including exchange.

REFERENCES

1. Haris M, Singh A, Cai K, Nath K, Crescenzi R, Kogan F, Hariharan H, Reddy R. MICEST: a potential tool for non-invasive detection of molecular changes in Alzheimer's disease. *J Neurosci Methods* 2013; 212:87–93.
2. Haris M, Nanga RP, Singh A, Cai K, Kogan F, Hariharan H, Reddy R. Exchange rates of creatine kinase metabolites: feasibility of imaging creatine by chemical exchange saturation transfer MRI. *NMR Biomed* 2012;25:1305–1309.

3. Cai K, Haris M, Singh A, Kogan F, Greenberg JH, Hariharan H, Detre JA, Reddy R. Magnetic resonance imaging of glutamate. *Nat Med* 2012;18:302–306.
4. Jia G, Abaza R, Williams JD, et al. Amide proton transfer MR imaging of prostate cancer: a preliminary study. *J Magn Reson Imaging* 2011; 33:647–654.
5. Basharat M, Jafar M, deSouza NM, Payne GS. Evaluation of short-TE (1)H MRSI for quantification of metabolites in the prostate. *NMR Biomed* 2014;27:459–467.
6. Swanson MG, Vigneron DB, Tabatabai ZL, Males RG, Schmitt L, Carroll PR, James JK, Hurd RE, Kurhanewicz J. Proton HR-MAS spectroscopy and quantitative pathologic analysis of MRI/3D-MRSI-targeted postsurgical prostate tissues. *Magn Reson Med* 2003;50: 944–954.
7. Bain AD. Chemical exchange in NMR. *Prog Nucl Magn Reson Spectrosc* 2003;43:63–103.
8. Kogan F, Singh A, Cai K, Haris M, Hariharan H, Reddy R. Investigation of chemical exchange at intermediate exchange rates using a combination of chemical exchange saturation transfer (CEST) and spin-locking methods (CESTRho). *Magn Reson Med* 2012;68:107–119.
9. McMahon MT, Gilad AA, Zhou J, Sun PZ, Bulte JW, van Zijl PC. Quantifying exchange rates in chemical exchange saturation transfer agents using the saturation time and saturation power dependencies of the magnetization transfer effect on the magnetic resonance imaging signal (QUEST and QUESP): pH calibration for poly-L-lysine and a starburst dendrimer. *Magn Reson Med* 2006;55:836–847.
10. Woessner DE, Zhang S, Merritt ME, Sherry AD. Numerical solution of the Bloch equations provides insights into the optimum design of PARACEST agents for MRI. *Magn Reson Med* 2005;53:790–799.
11. Woodward CK, Hilton BD. Hydrogen isotope exchange kinetics of single protons in bovine pancreatic trypsin inhibitor. *Biophys J* 1980; 32:561–575.
12. Weast RC, editor. *Handbook of chemistry and physics*. Boca Raton, FL: CRC Press; 1981.
13. Rohl CA, Baldwin RL. Exchange kinetics of individual amide protons in ^{15}N -labeled helical peptides measured by isotope-edited NMR. *Biochemistry* 1994;33:7760–7767.
14. Kavanagh JP. Sodium, potassium, calcium, magnesium, zinc, citrate and chloride content of human prostatic and seminal fluid. *J Reprod Fertil* 1985;75:35–41.
15. van Zijl PC, Jones CK, Ren J, Malloy CR, Sherry AD. MRI detection of glycogen in vivo by using chemical exchange saturation transfer imaging (glycoCEST). *Proc Natl Acad Sci U S A* 2007;104:4359–4364.
16. Terreno E, Stancanella J, Longo D, Castelli DD, Milone L, Sanders HM, Kok MB, Uggeri F, Aime S. Methods for an improved detection of the MRI-CEST effect. *Contrast Media Mol Imaging* 2009;4:237–247.
17. Gunther H. *NMR spectroscopy*. New York: John Wiley; 1980.
18. Pfau A, Perlberg S, Shapira A. The pH of the prostatic fluid in health and disease: implications of treatment in chronic bacterial prostatitis. *J Urol* 1978;119:384–387.
19. Blacklock NJ, Beavis JP. The response of prostatic fluid pH in inflammation. *Br J Urol* 1974;46:537–542.
20. Haris M, Cai K, Singh A, Hariharan H, Reddy R. In vivo mapping of brain myo-inositol. *Neuroimage* 2011;54:2079–2085.

SUPPORTING INFORMATION

Additional Supporting Information may be found in the online version of this article.

Supporting Figure S1. Structures of citrate (a) and spermine (b) showing protonation at physiologic pH, i.e., citrate has exchanging ^1H -O, expected to resonate just downfield of water (the hydroxyls in myo-inositol resonate at +0.8 to +0.6 ppm relative to water 20 for example), and spermine has ten exchanging ^1H nuclei which resonate at approximately 3.0 and 3.7 ppm relative to water (see Figure 1).